11th International Symposium on Turbulence and Shear Flow Phenomena (TSFP11)
Southampton, UK, July 30 to August 2, 2019

STRATIFIED TURBULENCE IN DISK WAKES

Karu Chongsiripinyo
Department of Mechanical and Aerospace Engineering
University of California at San Diego
La Jolla, CA 92093
kchongsi@eng.ucsd.edu

Sutanu Sarkar
Department of Mechanical and Aerospace Engineering
University of California at San Diego
La Jolla, CA 92093
sarkar@ucsd.edu

Abstract

The primary objective of this work is to investigate the evolution of turbulence in the core of decaying stratified wakes. Large-eddy simulations of unstratified and stratified flows past a disk are performed at $Re=U_bL_b/\nu$=50,000 and $Fr=U_b/NL_b=\infty$, 50,10 and 2; here, U_b is the free-stream velocity, L_b is the disk diameter, ν is the fluid kinematic viscosity, and N is the buoyancy frequency.

Unstratified wake-core turbulence is anisotropic in the near wake with $u'_y \approx u'_z > u'_x$. As the wake 'naturally' decays, turbulence gradually returns to isotropy. Buoyancy promotes anisotropy in stratified wakes: while $u'_x \approx u'_y \propto x^{-0.18}$, the vertical velocity fluctuation rate of decay is much larger at $u'_z \propto x^{-1}$. For high-Fr wakes, turbulence returns to isotropy before stratification sets in at $Nt_b \approx 1$ followed by a reversal along an axiysymmetric path towards the two-component (2C) point. On the other hand, at lower Fr, wake turbulence does not demonstrate a return to isotropy and progresses towards the 2C state along a non-axisymmetric trajectory.

Wake evolution can be categorized via a set of regimes discerned by the Froude number (Fr_h) of turbulence: weakly stratified turbulence (WST), intermediately stratified turbulence (IST), and strongly stratified turbulence (SST). These regimes are plotted in a phase space whose coordinates are Fr_h and $Re_hFr_h^2$ where Re_h is the Reynolds number of turbulence. WST begins when Fr_h decreases to $O(1)$, spans $1 \lesssim Nt_b \lesssim 5$ and, although the mean flow is strongly affected by buoyancy in WST, turbulence anisotropy is not. IST takes place at $Nt_b \approx 5$ once Fr_h decreases to $O(0.1)$. During IST, the mean flow has entered into the NEQ regime with a constant decay exponent, $U_0 \propto x^{-0.18}$, but turbulence is still in transition. SST commences when Fr_h decreases by another order of magnitude to $Fr_h \sim O(0.01)$. During SST that begins at $Nt_b \approx 20$, turbulence is strongly anisotropic ($u'_z \ll u'_y \sim u'_x$). Both $K^{1/2}$ and U_0 satisfy $x^{-0.18}$ decay during SST signifying that both turbulence and mean flow have arrived into the stratified non-equilibrium (NEQ) regime.

Introduction

Wakes are common in oceanic and atmospheric flows. Some examples are marine swimmers, underwater submersibles and flow over mountains and around islands. The ocean has stable density stratification that is mostly due to temperature variation in the vertical although salinity gradients also contribute to the stratification at some locations. Therefore, oceanic wakes inevitably encounter stratification. In the atmosphere, night-time and winter-time conditions have stable stratification that impacts the wakes of aerial vehicles.

Stratification is measured by $N^2 = -(g/\rho_0)\partial\rho/\partial z$ with the buoyancy frequency, N, typically varying between 10^{-3} s^{-1} at depth to 10^{-2} s^{-1} in the upper ocean. A submersible with characteristic length L_b that moves with speed U_b has a body-based Froude number, $Fr = U_b/NL_b$. Although the body Fr is typically large under cruise conditions, the local wake Fr decreases with increasing streamwise distance so that buoyancy eventually becomes important to wake dynamics. It is worth noting that body $Fr \leq O(1)$ is also possible in low-speed maneuvers.

Early experiments, as reviewed by Lin & Pao (1979), showed that stratification suppresses vertical motion, promotes the formation of horizontal coherent eddies, and enables propagation of internal gravity waves into the far field. The stratified wake of an axisymmetric body with $Fr \gg O(1)$ exhibits three distinct regions. The first region is the near wake (3D) where the wake spreads uniformly in the radial direction and turbulence behaves as it does in a homogeneous fluid. It is followed by a non-equilibrium (NEQ) regime identified by Spedding (1997) where there is an onset of buoyancy effects including anisotropy between horizontal and vertical motions, and conversion of stored potential energy to kinetic energy. The third quasi-two-dimensional (Q2D) region is characterized by the existence of vertically squashed two-dimensional eddies referred to as "pancake vortices".

Different from most previous studies that employ a temporal model that evolves assumed initial fields, the wake generator is explicitly included in the present work. Our previous body-inclusive simulations (Pal *et al.*, 2016, 2017;

Case	Fr	N_r	N_θ	N_x	L_r	L_θ	L_x
UNS	∞	364	256	4608	15.1	2π	125.5
F02	2	529	256	4608	80	2π	125.5
F10	10	529	256	4608	80	2π	125.5
F50	50	529	256	4608	80	2π	125.5

Table 1. Physical and numerical parameters used in the simulations. N_r, N_θ, and N_x are the number of nodes in the radial, azimuthal, and streamwise directions, respectively. All lengths are normalized by the disk diameter, L_b.

Chongsiripinyo *et al.*, 2017) that resolve both the near-body flow and the stratified far wake considered a sphere with low and moderate Fr, and a low $Re = 3700$. In contrast, the present work includes high Fr too, considers an order-of-magnitude larger $Re = 50,000$, and employs a disk as the wake generator. Without uncertainty introduced by assumed initial conditions, we address questions related to mean-wake power laws in both homogeneous and stratified fluids, as well as buoyancy effects on turbulence.

Formulation

The large-eddy simulation (LES) approach is employed with an immersed boundary method (extensively validated in previous work) to represent the disk. The non-dimensional governing equations (1-3) are numerically solved on a cylindrical coordinate system with a staggered-grid configuration.

$$\frac{\partial u_i}{\partial x_i} = 0, \tag{1}$$

$$\frac{\partial u_i}{\partial t} + u_j \frac{\partial u_i}{\partial x_j} = -\frac{\partial p}{\partial x_i} + \frac{1}{Re}\frac{\partial}{\partial x_j}\left[(1+\frac{\nu_s}{\nu})\frac{\partial u_i}{\partial x_j}\right] - \frac{1}{Fr^2}\rho_d \delta_{i3}, \tag{2}$$

$$\frac{\partial \rho}{\partial t} + u_j \frac{\partial \rho}{\partial x_j} = \frac{1}{RePr}\frac{\partial}{\partial_j}\left[(1+\frac{\kappa_s}{\kappa})\frac{\partial \rho}{\partial x_j}\right]. \tag{3}$$

The body Reynolds number is $Re{=}U_b L_b/\nu$ and the body Froude number is $Fr{=}U_b/NL_b$. The disk thickness of $0.01L_b$ is small. The Prandtl number, $Pr{=}\nu/\kappa$, that is the ratio of velocity and density (temperature) diffusivities is assumed to be unity. Additional variables from the modeled subgrid scales are subgrid kinematic viscosity, ν_s, and density diffusivity, κ_s. The Prandtl number based on these subgrid variables is also assumed to be unity. Details of the numerical algorithm can be found in Pal *et al.* (2017).

Parameters of the simulations are given in table 1. The grid spacing corresponds to high-resolution LES; e.g., beyond $x/L_b = 10$, the centerline $\Delta x_i/\eta$ (where η denotes the Kolmogorov length) is smaller than 10 and gradually decreases to about 6 at $x/L_b = 125$. $\Delta x_i/\eta$ is at worst ≈ 17 near the centerline at $x/L_b \approx 2.5$. Averaged drag coefficient in the unstratified case is found to be $C_d = 1.145$ comparable to the value of $C_d = 1.12$ in Fail *et al.* (1959).

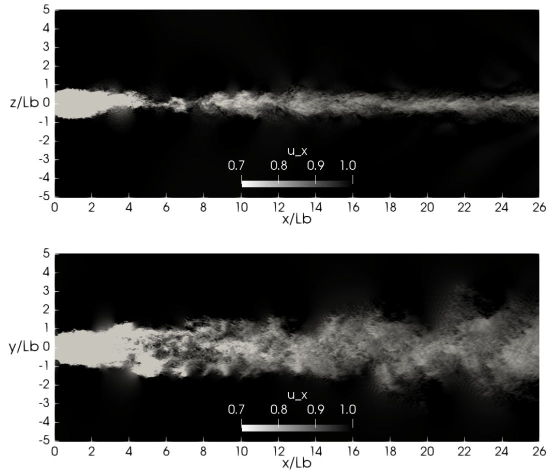

Figure 1. An instantaneous field of streamwise velocity (u_x) on a vertical ($x-z$) centerplane (top) and on a horizontal ($y-z$) centerplane (bottom) in the $Fr = 2$ case.

Results

At $Re = 5\times10^4$, instantaneous visualizations (e.g., figure 1) are suggestive of a turbulent wake even at the relatively high stratification of $Fr = 2$, albeit with distinct anisotropy between vertical and horizontal planes. Quantitative statistics (r.m.s. turbulence, dissipation rate, spectra) confirm the presence of broad-band wake turbulence. With increasing x/L_b, the flow transitions from weak buoyancy effects to a regime of stratified turbulence and eventually to viscous decay. The regime of stratified turbulence is distinguished by strong buoyancy effects on the large scales that coexists with an inertial subrange that exhibits down-scale energy cascade and survives in spite of buoyancy-dominated large scales, e.g., Riley & de Bruyn Kops (2003); Brethouwer *et al.* (2007); de Bruyn Kops & Riley (2019). At $Fr = 2$, the $Re = 5\times10^4$ disk wake is found to have a substantial range of x/L_b where there is stratified turbulence.

Mean and turbulent velocities

We first discuss the unstratified wake in a homogeneous fluid. Centerline mean streamwise velocity deficit (U_0) and turbulent velocity ($K^{1/2}$) are shown in figure 2. After the recirculation zone where $U_0 > U_b$ and there is an increase in turbulent kinetic energy (K) signifying turbulence establishment, U_0 decays in two stages with a break in slope at $x/L_b \approx 65$ in contrast to $K^{1/2}$ that decays with a single power law after $x \approx 10$. The first stage of $10 < x/L_b < 65$ exhibits $U_0 \propto x^{-0.9}$ and $L \propto x^{0.45}$ (not shown); L is a U_0-based axisymmetric wake width. This behavior is not due to low Re, and is similar to the approximately x^{-1} behavior found in previous examples: the sphere wake at $Re = 3700$ by Pal *et al.* (2017) and $Re = 10,000$ by Chongsiripinyo *et al.* (2019); and, fractal-plate wakes at $Re = 5000$ (DNS) and $Re = 50,000$ (laboratory experiment) by Dairay *et al.* (2015). The second stage takes place after $x/L_b \approx 65$ where U_0 exhibits a power law that is close to the classical round wake scaling $U_0 \sim K^{1/2} \precsim x^{-2/3}$ and $L \sim L_k \precsim x^{1/3}$; L_k is a K-based axisymmetric wake width.

In contrast to the monotone decay of U_0 seen in unstratified wakes, the $Fr = 2$ disk wake (F02 in figure 2) shows an increase of U_0 at $Nt = \pi$ ($x/L_b = \pi Fr$) which corresponds

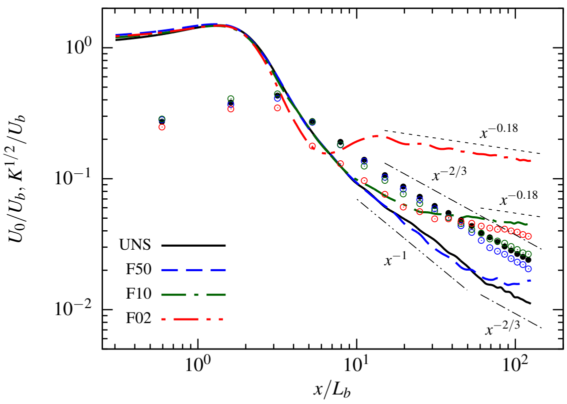

Figure 2. Histories of centerline mean streamwise defect velocity (U_0) shown in lines, and centerline turbulent characteristic velocity ($K^{1/2}$) plotted with symbols.

to the "oscillatory modulation" induced by lee waves that was identified in sphere wakes by Pal *et al.* (2017). The lee-wave modulation is weaker at $Fr = 10$ and insignificant at $Fr = 50$. After the initial adjustment to buoyancy, stratified wakes arrive at the non-equilibrium (NEQ) regime where $U_0 \propto x^{-0.18}$ is found to be different from $U_0 \propto x^{-0.25}$ characteristic of sphere wakes, e.g., Spedding (1997); Brucker & Sarkar (2010). The decay of $K^{1/2}$ also changes to $x^{-0.18}$ in the $Fr = 2$ case but much further from the body than the commencement of $U_0 \propto x^{-0.18}$ (compare the red circles with the red dashed line). Thus, stratification affects turbulence energetics much later than it does mean flow energetics.

Buoyancy-induced anisotropy

Cross-sectional contours of K for the UNS (top row), F10 (middle row), and F02 (bottom row) cases shown in figure 3 depict buoyancy-induced anisotropy in the spatial distribution of K. Depending on Fr and distance from the disk, stratification distorts the cross-sectional distribution of K from a circular isotropic shape in the unstratified wake into an elliptical distribution that is vertically thin (along 90^o and 270^o) but horizontally wide (along 0^o and 180^o). Initially, turbulence in the stratified wake core is less energetic relative to the unstratified case. Analysis of the turbulent kinetic energy budget (not shown) reveals that not only is turbulent production reduced but also K is initially expended to stir the density field, i.e., there is a negative buoyancy flux that augments turbulent potential energy. Restratification occurs later and is accompanied by positive turbulent buoyancy flux that causes turbulent kinetic energy to gain at the expense of potential energy. The enhanced TKE is seen in the late F02 wake (figure 3 (i)) and also in the late F10 and F02 wake from figure 2 where $K_{\mathrm{F10,F02}} > K_{\mathrm{UNS}}$ at sufficiently large x/L_b.

Anisotropy among the different wake r.m.s components is shown in figure 4. The UNS (unstratified) wake has axisymmetric normal stresses ($u'_y \approx u'_z$) during its entire evolution. The streamwise component (u'_x) is somewhat smaller than u'_y in the UNS near wake but progressively approaches the value of u'_y at increasing downstream distance as the mean velocity gradients continually decrease. Buoyancy-induced suppression of vertical motion progressively increases velocity anisotropy in the late wake. K is dominated by horizontal components that are comparable in magnitude; thus, $u'_x \approx u'_y$ follows the decay law of $K^{1/2} \propto x^{-0.18}$. Since the vertical r.m.s velocity fluctuation is found to evolve as $u'_z \propto x^{-1}$ (not shown), it follows that $u'_z/u'_y \sim u'_z/u'_x \approx x^{-0.82}$. A consequence for the F02 wake is that $u'_z/u'_y \sim u'_z/u'_x \sim O(0.1)$ by $x/L_b = 100$ (figure 4 top panel). Regarding the relative magnitude of the horizontal components (bottom panel of figure 4), u'_y/u'_x in the F10 and F50 wakes evolve similarly to the UNS wake which shows an approach to $u'_y \approx u'_x$. However in the F02 wake, the lateral component (u'_y) becomes larger than u'_x, a behavior that is consistent with the lateral meandering of the wake induced by coherent eddies in the horizontal plane.

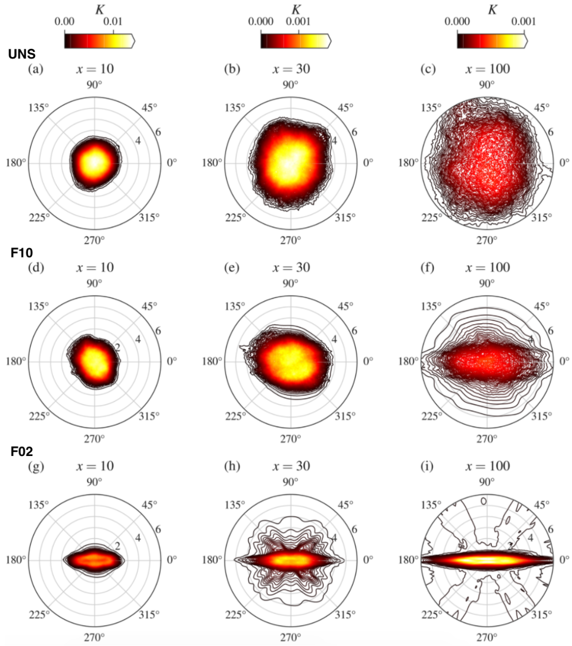

Figure 3. Visualization of cross-sectional contours of turbulent kinetic energy (K) for the UNS wake (top row), F10 wake (middle row), and F02 wake (bottom row) at $x/L_b = 10$ (left), $x/L_b = 30$ (center), and $x/L_b = 100$ (right).

Turbulence anisotropy is further assessed using the normalized deviatoric part, $b_{ij} = \langle u'_i u'_j \rangle / \langle u'_k u'_k \rangle - \delta_{ij}/3$, of the Reynolds stress tensor. Figure 5 shows the progression of turbulence anisotropy for cases F50, F10, and F02 in phase space, namely, the anisotropy invariant map or the Lumley triangle (Lumley & Newman, 1977) that is helpful to constrain turbulence models, e.g. Sarkar & Speziale (1990). The labels 'WST', 'IST', and 'SST' refer to different stages, to be described in the next section, of stratified turbulence that occur sequentially with increasing downstream distance. As buoyancy effects become stronger, the turbulence state changes. For instance, F02 wake turbulence deviates strongly from isotropy with increasingly large values of the anisotropy magnitude (η). Turbulence in the F02 wake tends towards the two-component line ($u'_z \ll$ the horizontal components) but is not necessarily axisymmetric since $u'_y > u'_x$.

It is useful to consider the UNS wake as a reference. UNS wake-core turbulence deviates away from its initial quasi-isotropic state (black filled circle) right behind the disk as the recirculation region develops and moves along the axisymmetric (axi) line with $\xi = -\eta$ (upward black vectors in figure 6). This axisymmetric path is consistent with $u'_z \approx u'_y > u'_x$ that was seen in figure 4. After reaching peak $\eta = 0.09$ at $x/L_b \approx 1.5$, UNS turbulence returns

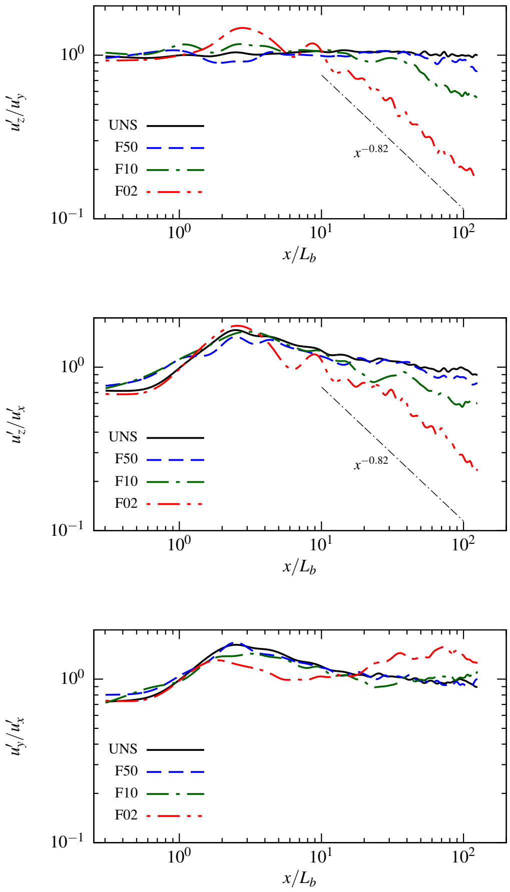

Figure 4. Ratio of vertical (u_z') to spanwise (u_y') velocity r.m.s fluctuations (top), ratio of vertical to streamwise (u_x') velocity r.m.s fluctuations (bottom), and ratio of spanwise to streamwise velocity r.m.s (bottom). The ratios are computed along wake centerlines.

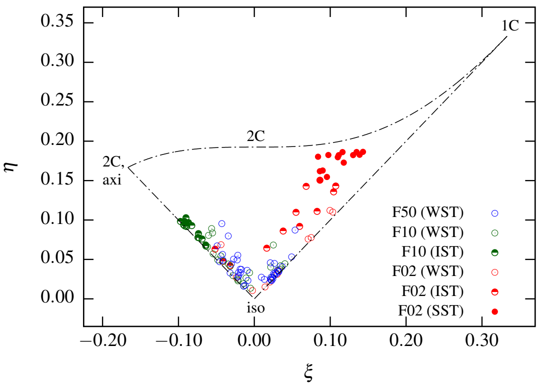

Figure 5. Anisotropy invariant map (Lumley triangle). Here, $\eta = (-II/3)^{1/2} = (b_{ij}b_{ij}/6)^{1/2}$ and $\xi = (III/2)^{1/3} = (b_{ij}b_{jk}b_{ki}/6)^{1/3}$.

(downward blue vectors in figure 6) towards the isotropic state. Turbulence remains quasi-isotropic in the late wake where both ξ and η are small (not shown). It is interesting to note that turbulence has approached quasi-isotropy at $x/L_b \approx 65$ where the wake decay law transitions from its initial power law to its eventual behavior of approximately $U_0 \propto x^{-2/3}$. F10 wake-core turbulence behaves similar to UNS in the region $x/L_b < 15$ (shown by black arrows in

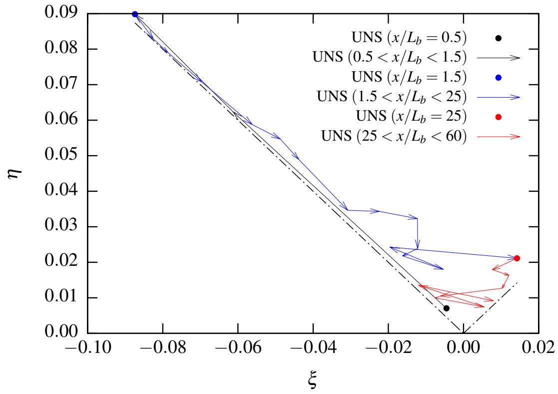

Figure 6. UNS: $\xi - \eta$ invariant map.

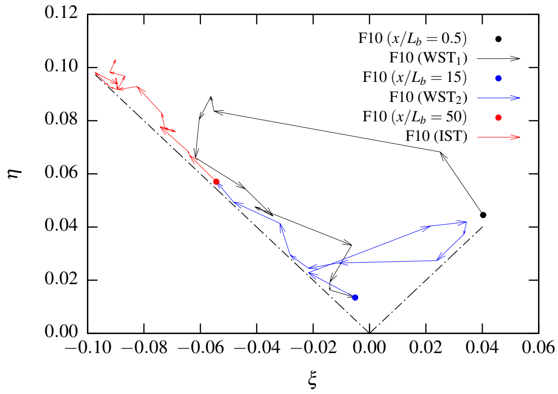

Figure 7. F10: $\xi - \eta$ invariant map.

figure 7); turbulence initially goes towards the axisymmetric state with $\xi = -\eta$, and then returns towards isotropic turbulence as the "natural decaying" wake relaxes from the effect of (decreasing) mean velocity gradients. However, stratification increases vertical mean shear of both horizontal velocity components that causes F10 wake-core turbulence to revert its trajectory towards the axisymmetric line and move upward, towards the axi-2C point, as u_z' continues to decrease relative to u_x', u_y'.

Turbulence in phase space

The $Fr_h - Re_h Fr_h^2$ phase-space map (Figure 8) shows the progression of each of the simulated cases through different stages of buoyancy influence on turbulence. The turbulent horizontal Froude number, $Fr_h = u_h'/NL_{Hk}$, is the ratio of the buoyancy timescale (N^{-1}) to the turbulent horizontal timescale (L_{Hk}/u_h'), and is a measure of the strength of buoyancy effects on the energy-containing scales; a decrease in Fr_h implies an increase in the relative strength of buoyancy. Large scales of motion are preferentially affected by buoyancy. More precisely, eddies with size larger than the Ozmidov length (l_o defined by Eq. 4) are restrained from overturning by buoyancy. Fr_h can also be interpreted based on length scales using $\varepsilon \sim u_h'^3/L_{Hk}$ that leads to $Fr_h = (l_o/L_{Hk})^{2/3}$. The wakes pass from a state of weak buoyancy (WB) to stratified turbulence (ST) at $Fr_h = 1$ when the large-eddy lengthscale (L_{Hk}) becomes equal to the Ozmidov lengthscale (l_o). Figure 8 shows that F50 and F10 wakes experience a WB stage before passing into the ST stage, unlike the F02 wake where turbulence near the body is already in the ST stage.

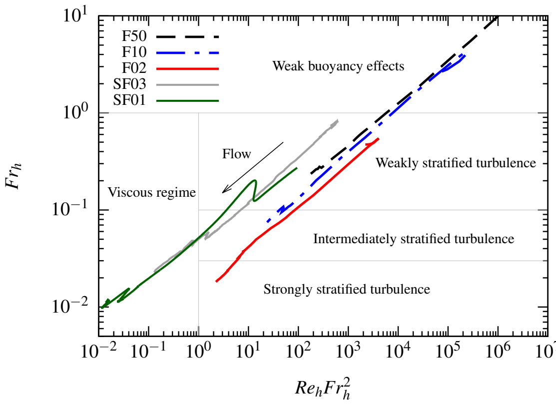

Figure 8. Evolution of the simulated wakes in $Fr_h - Re_h Fr_h^2$ phase space computed using centerline values of Fr_h and $Re_h Fr_h^2$. SF03 and SF01 cases are LES of stratified flow past a sphere of Chongsiripinyo & Sarkar (2017) at $Re = 10^4$ with $Fr = 3$ and $Fr = 1$, respectively.

As the wake progresses in the ST stage, $Fr_h = (l_o/L_{Hk})^{2/3}$ progressively decreases and the subrange of length scales ($L_{Hk} < l < l_o$) that is affected by buoyancy expands. The other quantity in the phase-space plot is $Re_h Fr_h^2$ that helps identify if the flow, despite the expanding range of eddies controlled by buoyancy, contains a subrange of length scales that continues to exhibit turbulent motions dominated by inertia. Billant & Chomaz (2001) introduced $Re_h Fr_h^2 > 1$ as a condition that ensures that viscous effects do not directly affect turbulent motions, and Riley & de Bruyn Kops (2003) relate $Re_h Fr_h^2$ to an inverse Richardson number of fluctuating motions so that $Re_h Fr_h^2 > O(1)$ implies the possibility of local shear instability. In the present work, Re_h is computed as $Re_h = u'_h L_{Hk}/\nu$. It is worth noting that $Re_h Fr_h^2$ can be related to the buoyancy Reynolds number, denoted by Re_b, via the inviscid estimate dissipation scaling, $\varepsilon \sim u_h'^3/L_{Hk}$. Re_b can be expressed as a ratio of inertial and viscous forces,

$$Re_b = \frac{u_o l_o}{\nu}; \quad u_o = \left(\frac{\varepsilon}{N}\right)^{1/2}, \quad l_o = \left(\frac{\varepsilon}{N^3}\right)^{1/2}, \qquad (4)$$

i. e., the Reynolds number of Ozmidov-scale eddies. Eddies with size larger than the Ozmidov length (l_o) are prevented by buoyancy from overturning. Since $Re_b = (l_o/\eta)^{4/3}$ where $\eta = (\nu^3/\varepsilon)^{1/4}$ is the Kolmogorov scale, it follows that when $Re_b \gg 1$ there is a large scale separation between the Ozmidov and the Kolmogorov scales which is necessary for the existence of an inertial subrange that is unaffected by either buoyancy or viscous forces.

As noted previously in this section, the wakes pass from a state of weak buoyancy (WB) to stratified turbulence (ST) at $Fr_h = 1$ when L_{Hk} becomes equal to l_o. Figure 9 (top) shows that Fr_h decreases to 1 at about the first buoyancy adjustment period ($Nt_b \approx 1$) in the high-Fr wakes (F50 and F10) while the lower-Fr wakes start with $Fr_h < 1$. Figure 9 (bottom) shows that at $Nt_b = 1$, the $Re = 50{,}000$ disk-wake turbulence has $Re_h Fr_h^2 \sim O(10^3)$ while the $Re = 10{,}000$ sphere-wake turbulence of Chongsiripinyo & Sarkar (2017) has a much smaller $Re_h Fr_h^2 \sim O(10^2)$.

Stratified wake turbulence can be further subcategorized into 3 regimes: weakly stratified turbulence (WST), intermediately stratified turbulence (IST), and strongly stratified turbulence (SST) as marked in figure 8. In the WST stage that commences at $Nt_b \approx 1$, the effect of buoyancy on the mean flow (as inferred from the U_0 evolution in figure 2) is significant but its effect on turbulence is not. In particular, turbulence anisotropy is hardly affected in the WST regime. The value of Fr_h has to decrease from unity by almost an order of magnitude before there is a trend of increasing turbulence anisotropy associated with r.m.s in the horizontal continually becoming larger than in the vertical.

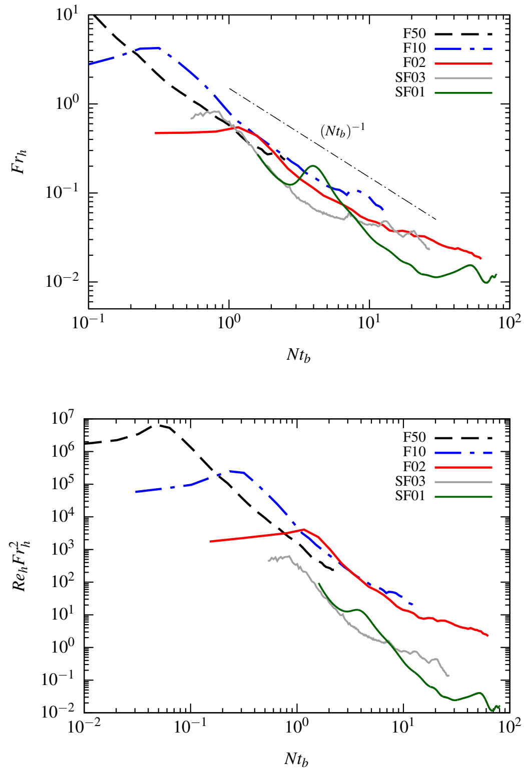

Figure 9. Evolution of phase-space parameter Fr_h (top) and $Re_h Fr_h^2$ (bottom).

As seen in figure 4, turbulence anisotropy increases (u'_z/u'_y and u'_z/u'_x decrease) in $Fr = 2, 10$ wakes at $x/L_b \approx 10, 50$, respectively, or $Nt_b \approx 5$ in both wakes. Based on the corresponding values of $Fr_h(Nt_b = 5)$ in figure 9, this suggests that WST transitions at $Fr_h \sim O(0.1)$ to a regime of intermediately stratified turbulence (IST) that is distinguished by progressively increasing turbulence anisotropy. The final stage of strongly stratified turbulence (SST) is based on Fr_h decreasing to $\sim O(0.01)$. In particular, we consider SST to commence at $Fr_h = 0.03$, based on the value of vertical turbulent Froude number $Fr_v = u'_h/Nl_v$, where we find that $l_v = u'_h/\partial_z u'_h$ approaches an $O(1)$ constant. It is worth noting that $Fr_h = 0.03$ is close to the prediction of Lindborg (2006) that the critical horizontal Froude number $Fr_{h,crit} = 0.02$. Only the $Fr = 2$ wake is able to cross the $Fr_h = 0.03$ boundary to access the SST regime. The entry of the F02 wake into the SST regime occurs at $Nt_b = 20$ where $Fr_h = 0.03$ from figure 9 (top).

Summary and conclusions

Large-eddy simulations of unstratified and stratified flows past a disk are performed at Re=$U_b L_b/\nu$=50,000 and

Fr=U_b/NL_b=$\infty, 50, 10, 2$; here, U_b is the free-stream velocity, L_b is the disk diameter, ν is the fluid kinematic viscosity, and N is the buoyancy frequency. The objective is to investigate the effects of buoyancy on evolution of wake turbulence as well as to ascertain power laws satisfied by the wake characteristic velocities in both homogeneous and stratified fluids.

In the unstratified wake, it is found that the mean streamwise velocity deficit (U_0) decays in two stages: $U_0 \propto x^{-0.9}$ during $10 < x/L_b < 65$, and $U_0 \precapprox x^{-2/3}$ after $x/L_b \approx 65$. The turbulent characteristic velocity, taken as $K^{1/2}$ with K the turbulent kinetic energy (TKE), satisfies $K^{1/2} \precapprox x^{-2/3}$ after $x/L_b \approx 10$. In the stratified wakes, the initial rates of U_0 decay deviate from the unstratified counterpart at $Nt_b \approx 1$, equivalently $x/L_b = Fr$. Thus, in none of the simulated stratified wakes is the first regime of quasi-unstratified behavior sufficiently long to exhibit the classical $U_0 \propto x^{-2/3}$ behavior. After the non-equilibrium regime (NEQ) is established, it is found that $U_0 \sim K^{1/2} \propto x^{-0.18}$.

Wake-core turbulence is found to initially be anisotropic in both unstratified and high-Fr wakes where the streamwise component (u'_x) is smaller than the other two components (u'_y, u'_z). The $\xi - \eta$ invariant map (Lumley triangle) shows that both UNS and F10 wake turbulence, after reaching peak anisotropy magnitude in the near wake, tend to return to isotropy along the axisymmetric branch ($\xi = -\eta$). While the UNS wake turbulence remains quasi-isotropic, the F10 wake turbulence reverts to anisotropy and progresses towards the 2C state ($u'_z \ll u'_x, u'_y$) again following the axisymmetric branch. At the stronger stratification of $Fr = 2$, the behavior is different. F02 wake turbulence does not exhibit an intermediate phase of return to isotropy but continually moves towards a 2C state, and takes a path that is no longer axisymmetric.

The evolution of stratified wakes can be categorized via a turbulence-based set of regimes delineated by the turbulent Froude number ($Fr_h = u'_h/NL_{Hk}$; u'_h and L_{Hk} are r.m.s horizontal velocity and TKE-based horizontal wake width). *Weakly stratified turbulence* (WST) begins when Fr_h decreases to $O(1)$, spans $1 \lesssim Nt_b \lesssim 5$ and, while the mean flow is strongly affected by buoyancy in WST, turbulence anisotropy is not. *Intermediately stratified turbulence* (IST) commences at $Nt_b \approx 5$ once Fr_h decreases to $O(0.1)$. During IST, the mean flow has entered into the NEQ regime with a constant decay exponent, $U_0 \propto x^{-0.18}$, but turbulence is still in transition. *Strongly stratified turbulence* (SST) commences when Fr_h decreases by another order of magnitude to $Fr_h \sim O(0.01)$. During SST that begins at $Nt_b \approx 20$, turbulence is strongly anisotropic ($u'_z \ll u'_y \sim u'_x$). Both $K^{1/2}$ and U_0 satisfy $x^{-0.18}$ decay during SST signifying the official arrival of the NEQ regime for both turbulence and mean flow.

Buoyancy preferentially affects the large eddies. The state of stratified turbulence is plotted in a two-dimensional phase space where the Fr_h coordinate measures the effect of buoyancy on the large eddies of turbulence and the $Fr_h Re_h^2$ coordinate measures the Reynolds number of the largest eddy that is not directly affected by buoyancy. In phase space, all disk wakes at $Re = 50{,}000$ take similar paths but the F02 wake is the only one in the present simulations that has evolved to $Nt_b > 20$, sufficient to exhibit the SST stage.

Acknowledgments

We gratefully acknowledge the support of ONR Grant No. N00014-15-1-2718. Computational resources were provided by the Department of Defense High Performance Computing Modernization Program.

REFERENCES

Billant, P. & Chomaz, J.-M. 2001 Self-similarity of strongly stratified inviscid flows. *Phys. Fluids* **13** (6), 1645–1651.

Brethouwer, G., Billant, P., Lindborg, E. & Chomaz, J.-M. 2007 Scaling analysis and simulation of strongly stratified turbulent flows. *J. Fluid Mech.* **585**, 343–368.

Brucker, K. A. & Sarkar, S. 2010 A comparative study of self-propelled and towed wakes in a stratified fluid. *J. Fluid Mech.* **652**, 373–404.

de Bruyn Kops, S. M. & Riley, J. J. 2019 The effects of stable stratification on the decay of initially isotropic homogeneous turbulence. *J. Fluid Mech.* **860**, 787–821.

Chongsiripinyo, K., Pal, A. & Sarkar, S. 2017 On the vortex dynamics of flow past a sphere at Re= 3700 in a uniformly stratified fluid. *Phys. Fluids* **29** (2), 020704.

Chongsiripinyo, K., Pal, A. & Sarkar, S. 2019 Scaling laws in the axisymmetric wake of a sphere. In *Direct and Large-Eddy Simulation XI*, pp. 439–444. Springer.

Chongsiripinyo, K. & Sarkar, S. 2017 Effect of stratification on turbulent wake behind a sphere at Re = 10,000. In *Tenth International Symposium on Turbulence and Shear Flow Phenomena (TSFP10), July 6-9, 2017, Swissotel, Chicago-IL, USA*.

Dairay, T., Obligado, M. & Vassilicos, J.C. 2015 Non-equilibrium scaling laws in axisymmetric turbulent wakes. *J. Fluid Mech.* **781**, 166–195.

Fail, R., Eyre, R. C. W. & Lawford, J. A. 1959 *Low-speed experiments on the wake characteristics of flat plates normal to an air stream*. HM Stationery Office.

Lin, J. T. & Pao, Y. H. 1979 Wakes in stratified fluids. *Ann. Rev. Fluid Mech.* **11**, 317–338.

Lindborg, E. 2006 The energy cascade in a strongly stratified fluid. *J. Fluid Mech.* **550**, 207–242.

Lumley, John L & Newman, Gary R 1977 The return to isotropy of homogeneous turbulence. *Journal of Fluid Mechanics* **82** (1), 161–178.

Pal, A., Sarkar, S., Posa, A. & Balaras, E. 2016 Regeneration of turbulent fluctuations in low-Froude number flow over a sphere at Reynolds number of 3700. *J. Fluid Mech.* **804 R2**, 1–11.

Pal, A., Sarkar, S., Posa, A. & Balaras, E. 2017 Direct numerical simulation of stratified flow past a sphere at a subcritical Reynolds number of 3700 and moderate froude number. *J. Fluid Mech.* **826**, 5–31.

Riley, J. J. & de Bruyn Kops, S. M. 2003 Dynamics of turbulence strongly influenced by buoyancy. *Phys. Fluids* **15** (7), 2047–2059.

Sarkar, S. & Speziale, C. G. 1990 A simple nonlinear model for the return to isotropy in turbulence. *Physics of Fluids A: Fluid Dynamics* **2** (1), 84–93.

Spedding, G. R. 1997 The evolution of initially turbulent bluff-body wakes at high internal Froude number. *J. Fluid Mech.* **337**, 283–301.